Available online at www.sciencedirect.com

ScienceDirect

IFAC Papers Online CONFERENCE PAPER ARCHIVE

IFAC PapersOnLine 50-1 (2017) 2175–2180

Analytic Derivation of Battery SOC Estimation Error under Sensor Noises

Xinfan Lin *

* *Department of Mechanical and Aerospace Engineering, University of California, Davis, Davis, CA 95616 USA (e-mail: lxflin@ucdavis.edu).*

Abstract: It is well recognized that voltage and current sensor noises are one of the major sources of battery state of charge (SOC) estimation errors. However, quantitative relationship between the estimation error and sensing noises remains to be established systematically. This paper is devoted to filling this critical gap by deriving the analytic expression of the SOC estimation error under sensing noises. The considered sensing noises include both bias and variance. The derivation is based on a Kalman filter and an equivalent circuit battery model. The obtained analytic expressions can be conveniently used to evaluate the robustness and reliability of SOC estimation as well as guide observer design.

Keywords: Lithium Ion Battery, State of Charge Estimation, Sensor Bias, Sensor Variance, Estimation Error

1. INTRODUCTION

Estimation of battery states and parameters is a critical function of the battery management system (BMS). These states and parameters usually include the state of charge (SOC), which stands for the energy storage level of a battery cell or system, resistance, and capacity among others. Numerous methods have been proposed to perform the estimation. For example, the basic method for SOC estimation is coulomb counting, which integrates the current over time to obtain the remaining energy in the battery (Cadirci and Ozkazanc (2004) and Ng et al. (2004)). The results of coulomb counting, however, are easily corrupted by the initial SOC error and the bias in current sensing. In order to address these issues, model-based methods have been studied extensively for both state and parameter estimation, which combines a battery model and current and voltage measurement to improve the estimation accuracy. These methods include but are not limited to extended Kalman filtering (Plett (2004); Domenico et al. (2010); Fang et al. (2014)), moving horizon observer (Lin et al. (2013b, 2014b)), least squares method (Plett (2011); Lin et al. (2013a); Zhao and de Callafon (2013)), back-stepping PDE observer (Moura et al. (2014); Perez and Moura (2015)), and Lyapunov-based methods (Dey et al. (2015)).

Since all estimation algorithms need to use either or both of the voltage and current measurements, sensor noises, including bias and variance, will affect the estimation accuracy inevitably. Sensor bias refers to the deviation of the mean measurement value from the true value, while sensor variance refers to the variation of measurement values among samples. Many research efforts have been devoted to reducing the estimation error caused by sensor noises. Various estimation algorithms have been designed to optimize the estimation accuracy subject to voltage and (process) noise variance, such as the extended Kalman filter (EKF) and particle filtering (PF). Detection and correction of voltage and current sensor bias have also been explored in many research efforts (Zhao et al. (2016); Liu et al. (2016)).

However, in reality, it is often impossible to eradicate the impact of sensor noise, sometimes not even mitigating it. Regarding sensor variance, algorithms such as EKF need to assume known noise characteristics and could only alleviate the noise effect against that of the process noise. For sensor bias, as pointed out by Zhao et al. (2016) based on observability analysis, estimating (and hence correcting) sensor bias from the measurement data would require the battery open circuit voltage to satisfy certain condition.

Under such circumstance, it is important to evaluate the impact of sensor noises on estimation accuracy so as to predict the observer performance or guide observer design/sensor selection. Previously, the impact of voltage sensor variance has been studied quantitatively in Sharma and Fathy (2014) and Lin and Stefanopoulou (2015). Specifically, the variance of estimation errors was derived analytically based on an equivalent circuit battery model in Lin and Stefanopoulou (2015) and Lin (2016). The deviation of battery parameter estimation under sensor bias has been simulated in Yuan et al. (2015). However, a systematic and analytic analysis of estimation accuracy considering both sensor bias and variance is still missing. This paper is devoted to filling this important gap in the field.

The contributions of this work include the following aspects. First, the mean and variance of SOC estimation errors under sensor bias and variance are derived analytically. The derivation is based on a Kalman filter and an equivalent circuit battery model, which are the most widely adopted method and model for battery state esti-

10.1016/j.ifacol.2017.08.277

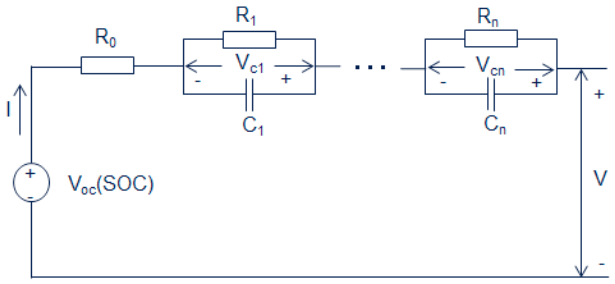

Fig. 1. Schematic of an equivalent circuit battery model

mation. Second, the contributing factors to the estimation errors are identified based on the analytic expressions. In addition, it is shown that there is a tradeoff between suppressing the SOC estimation bias and the variance regarding observer gain design. The methodology can be used to analyze the estimation errors of other battery states and parameters.

2. PROBLEM FORMULATION

In this section, the model, sensor noises, and SOC estimation error are defined.

2.1 Equivalent Circuit Battery Model

An equivalent circuit model (Hu et al. (2012); Lin et al. (2014a)) is used for analysis in this paper. Its schematic is shown in Fig. 1.

The discrete-time equivalent circuit model takes the form

$$\begin{aligned} SOC_{k+1} =& SOC_k + \frac{I_k \Delta t}{C_{bat}} \\ V_{cj,k+1} =& e^{-\frac{\Delta t}{R_j C_j}} V_{cj,k} + R_j (1 - e^{-\frac{\Delta t}{R_j C_j}}) I_k, \\ V_k =& g(SOC_k) + \sum_j^n V_{cj,k} + I_k R_0. \end{aligned} \tag{1}$$

The first equation computes the battery SOC based on coulomb counting, where I stands for current input (positive for charging), Δt is the sampling interval, C_{bat} is the capacity, and the subscript k denotes the time step. The second equation represents a series of equivalent R-C pairs used to capture the transient voltage dynamics, with voltage V_{cj} and parameters R_j and C_j for each pair j. The third equation calculates the terminal voltage by summing up a nonlinear SOC-dependent open circuit voltage, $g(SOC_k)$, V_{cj}, and an ohmic voltage loss over the battery resistance R_0.

2.2 Sensor Noise and SOC Estimation Error

The considered voltage sensor noise includes a constant bias, ΔV, and a random part δV_k, which is independently and identically distributed (i.i.d.) among samples with zero mean and variance σ_V^2. The true battery voltage at each time step is denoted as V_k^*. The voltage measurement V_k^m is then

$$V_k^m = V_k^* - \Delta V - \delta V_k. \tag{2}$$

For current noise, only a constant current bias ΔI is considered in the subsequent derivation for the following two reasons. First, the impact of the zero-mean random current noise on SOC calculation is negligible since its sum over time is zero. Second, the impact on voltage is also minimal due to the typically small resistance of lithium ion battery. The current measurement I_k^m is then

$$I_k^m = I_k^* - \Delta I. \tag{3}$$

Based on (1), the measured battery voltage can be represented as

$$V_k^m = g(SOC_k^*) + \sum_j^n V_{cj,k}^* + I_k^* R_0 - \Delta V - \delta V_k, \tag{4}$$

where the superscript $*$ denotes the true value.

Suppose now that a model-based observer is designed to estimate battery SOC based on (1). The voltage estimate of the observer using the measured current value is

$$\hat{V}_k = g(\hat{SOC}_k) + \sum_j^n \hat{V}_{cj,k} + (I_k^* - \Delta I) R_0, \tag{5}$$

where the superscript $\hat{}$ denotes the estimated value. The SOC estimation error is defined as

$$\Delta SOC_k = SOC_k^* - \hat{SOC}_k. \tag{6}$$

Most observers find the SOC estimate by matching the estimated voltage with the measurement. Since the equivalent circuit model is observable (see Zhao et al. (2016)), if $V^m = V^*$, $I^m = I^*$, and the model captures the voltage exactly, $\hat{V} = V^m$ will give $\hat{SOC} = SOC^*$. However, in the presence of sensor and model uncertainty, the solved $\hat{SOC}$ will not match the true value. Previously, the SOC estimation error ΔSOC induced by model parameter mismatch has been investigated in Lin et al. (2011). This paper focuses on studying ΔSOC under sensor noises.

3. DERIVATION OF SOC ESTIMATION ERROR

In this section, the analytic expressions of SOC estimation error ΔSOC under voltage sensor bias ΔV, voltage sensor variance δV_k, and current sensor bias ΔI are derived for the (extended) Kalman filter. A brief overview of EKF is given first, and the derivation is then performed based on the error dynamics.

3.1 SOC Estimation Using Kalman Filter

When Kalman filter is applied for battery SOC estimation, at each time instant k, SOC is first predicted by using model (1) and current measurement,

$$\begin{aligned} \hat{SOC}_k^- =& \hat{SOC}_{k-1} + \frac{I_{k-1}^m \Delta t}{Q}, \\ P_k^- =& P_{k-1} + Q \end{aligned} \tag{7}$$

where P is the (estimated) SOC estimation covariance, Q is the process noise variance assumed by the Kalman filter, and the superscript $^-$ denotes the model prediction. The estimates are then updated based on the voltage prediction error,

$$\begin{aligned} \hat{SOC}_k &= \hat{SOC}_k^- + L_k (V_k^m - \hat{V}_k^-), \\ P_k &= (1 - L_k \hat{\alpha}_k) P_k^- \end{aligned} \tag{8}$$

where the feedback gain is calculated as,

$$L_k = P_k^- \hat{\alpha}_k^T (\hat{\alpha}_k P_k^- \hat{\alpha}_k^T + \sigma_V^2)^{-1}. \tag{9}$$

In (8) and (9), $\hat{\alpha}_k$ is the gradient of $g(SOC)$ evaluated at $S\hat{O}C_k^-$,

$$\hat{\alpha}_k = \left.\frac{\partial g}{\partial SOC}\right|_{S\hat{O}C_k^-}. \tag{10}$$

3.2 Mean and Variance of SOC Estimation Error under Kalman Filter

A recursive form of $S\hat{O}C_k$ can be obtained by combining (7) and (8) as

$$S\hat{O}C_k = S\hat{O}C_{k-1} + \frac{I_{k-1}^m \Delta t}{C_{bat}} + L_k(V_k^m - \hat{V}_k^-), \tag{11}$$

where

$$\hat{V}_k^- = g(S\hat{O}C_k^-) + \sum_j^n \hat{V}_{cj,k} + I_k^m R_0. \tag{12}$$

The voltage prediction error is then calculated based on (4) and (12),

$$\begin{aligned} V_k^m - \hat{V}_k^- = \\ g(SOC_k^*) - g(S\hat{O}C_k^-) + \Delta I R_0 - \Delta V - \delta V_k. \end{aligned} \tag{13}$$

It is assumed here that $\sum_j^n V_{cj,l}^* = \sum_j^n \hat{V}_{cj,l}$ since the difference of the two caused by current bias ΔI is minimal. We then approximate

$$\begin{aligned} & g(SOC_k^*) - g(S\hat{O}C_k^-) \\ & \approx g(SOC_{k-1}^* + \frac{I_{k-1}^* \Delta t}{C_{bat}}) - g(S\hat{O}C_{k-1} + \frac{I_{k-1}^m \Delta t}{C_{bat}}) \\ & \approx g(SOC_{k-1}^*) + \alpha_k \frac{I_{k-1}^* \Delta t}{C_{bat}} - g(S\hat{O}C_{k-1}) - \alpha_k \frac{I_{k-1}^m \Delta t}{C_{bat}} \\ & \approx \alpha_k \Delta SOC_{k-1} + \alpha_k \frac{\Delta I \Delta t}{C_{bat}}. \end{aligned} \tag{14}$$

This approximation holds when $S\hat{O}C_k$ is not too far away from SOC_k^*.

By substituting (13) and (14) into (11), we have

$$\begin{aligned} S\hat{O}C_k = S\hat{O}C_{k-1} + \frac{I_{k-1}^m \Delta t}{C_{bat}} + \\ L_k(\alpha_k \Delta SOC_{k-1} + \alpha_k \frac{\Delta I \Delta t}{C_{bat}} + \Delta I R_0 - \Delta V - \delta V_k). \end{aligned} \tag{15}$$

Meanwhile, the true SOC is computed as

$$SOC_k^* = SOC_{k-1}^* + \frac{I_{k-1}^* \Delta t}{C_{bat}}. \tag{16}$$

A recursive form of the estimation error ΔSOC can be obtained by subtracting (15) from (16),

$$\begin{aligned} \Delta SOC_k = (1 - \alpha_k L_k)\Delta SOC_{k-1} + (1 - \alpha_k L_k)\frac{\Delta I \Delta t}{C_{bat}} \\ + L_k(\Delta V + \delta V_k - \Delta I R_0). \end{aligned} \tag{17}$$

It is noted here that in order for the error dynamics to be stable, the feedback gain L_k needs to satisfy

$$0 < L_k < \frac{2}{\alpha_k}. \tag{18}$$

When the initial SOC estimation error is ΔSOC_0, the expression for ΔSOC_k is

$$\begin{aligned} \Delta SOC_k = & \prod_{i=0}^{k-1}(1 - \alpha_i L_i)\Delta SOC_0 \\ & + \sum_{i=0}^{k-1}\left\{\left[(1 - \alpha_i L_i)\frac{\Delta I \Delta t}{C_{bat}} + L_i(\Delta V + \delta V_i - \Delta I R_0)\right]\right. \\ & \left. \cdot \prod_{m=i+1}^{k-1}(1 - \alpha_m L_m)\right\}. \end{aligned} \tag{19}$$

Since δV is an i.i.d. zero-mean random variable with variance σ_V^2, the expectation and variance of ΔSOC_k are

$$\begin{aligned} E(\Delta SOC_k) = & \prod_{i}^{k-1}(1 - \alpha_i L_i)\Delta SOC_0 \\ & + \sum_{i=0}^{k-1}\left\{\left[(1 - \alpha_i L_i)\frac{\Delta I \Delta t}{C_{bat}} + L_i(\Delta V - \Delta I R_0)\right]\right. \\ & \left. \cdot \prod_{m=i+1}^{k-1}(1 - \alpha_m L_m)\right\}. \\ \sigma^2(\Delta SOC_k) = & \sum_{i=0}^{k-1}\left\{L_i \prod_{m=i+1}^{k-1}(1 - \alpha_m L_m)\right\}^2 \sigma_V^2. \end{aligned} \tag{20}$$

Furthermore, if $g(SOC)$ is linear with a constant slope α, the feedback gain will converge to a constant L, and (20) is reduced to

$$\begin{aligned} E(\Delta SOC_k) = & (1 - \alpha L)^k \Delta SOC_0 + \frac{1 - (1 - \alpha L)^k}{\alpha L} \\ & \cdot \left[(1 - \alpha L)\frac{\Delta I \Delta t}{C_{bat}} + L(\Delta V - \Delta I R_0)\right] \\ \sigma^2(\Delta SOC_k) = & L^2 \frac{1 - (1 - \alpha L)^{2k}}{1 - (1 - \alpha L)^2}\sigma_V^2. \end{aligned} \tag{21}$$

When $k \to \infty$ and L satisfies (18), (21) converges to

$$\begin{aligned} E(\Delta SOC) \to & \frac{\Delta I \Delta t}{\alpha L C_{bat}} + \frac{\Delta V - \Delta I R_0}{\alpha} - \frac{\Delta I \Delta t}{C_{bat}} \\ \sigma^2(\Delta SOC) \to & \frac{\sigma_V^2}{\frac{2\alpha}{L} - \alpha^2}. \end{aligned} \tag{22}$$

The expectation $E(\Delta SOC)$ represents the bias of SOC estimation under δV, ΔV, and ΔI. The variance $\sigma^2(\Delta SOC)$ reflects the spread of the SOC estimation errors around the estimation bias. Following observations can be made from (22) and the derivation process.

(1) In the presence of sensing bias ΔV and ΔI, the observer gain L needs to be constrained by the OCV slope α according to (18) to guarantee stability. [1] Under such circumstance, the estimation bias $E(\Delta SOC_k)$ and variance $\sigma^2(\Delta SOC_k)$ are bounded. Furthermore, if α and L are constant, $E(\Delta SOC_k)$ and $\sigma^2(\Delta SOC_k)$ will converge to (22) asymptotically.
(2) The asymptotic estimation bias $E(\Delta SOC)$ first includes a gain-dependent term, $\frac{\Delta I \Delta t}{\alpha L C_{bat}}$, which is induced by the current sensing bias ΔI. This term increases with ΔI and decreases as α and L grows. It means that large sensor bias and flat OCV curve

[1] It can be proven that such condition is guaranteed by the Kalman filter.

will lead to large SOC estimation bias. Applying large gain L could reduce this estimation bias. Since L is constrained by (18), this term varies between

$$\frac{|\Delta I|\Delta t}{2C_{bat}} < \left|\frac{\Delta I \Delta t}{\alpha L C_{bat}}\right| < +\infty. \quad (23)$$

The lower bound $\frac{|\Delta I|\Delta t}{2C_{bat}}$ is approached when L is close to $\frac{2}{\alpha}$. The upper bound $(+\infty)$ is attained when $L = 0$, corresponding to the case of coulomb counting where the SOC estimation error keeps accumulating over time due to current bias.

(3) The asymptotic bias $E(\Delta SOC)$ further includes a gain-independent term, $\frac{\Delta V - \Delta I R_0}{\alpha} - \frac{\Delta I \Delta t}{C_{bat}}$, which is not affected by the observer gain. This term is proportional to the magnitude of sensing biases ΔV and ΔI and inversely proportional to the OCV slope α. It indicates the fundamental estimation bias induced by sensing biases that cannot be mitigated by KF gain calibration.

(4) The asymptotic estimation error variance $\sigma^2(\Delta SOC)$ depends on the voltage noise variance σ_V^2, OCV slope α, and the observer gain L. Small σ_V^2 and large α reduce the estimation variance. High L increases the variance as enhanced voltage feedback amplifies the effect of δV. With L subject to (18), the estimation variance varies within

$$0 < \sigma^2(\Delta SOC) < +\infty. \quad (24)$$

The lower bound 0 is attained when $L = 0$, corresponding to the case of coulomb counting where voltage feedback is not used. The upper bound $(+\infty)$ is approached when L is close to $\frac{2}{\alpha}$.

In summary, within the stable range in (18), increasing the observer gain could reduce the SOC estimation bias induced by the current sensing bias. But this is achieved at the cost of amplifying the error variance caused by the voltage sensing variance. The estimation bias induced by voltage sensing bias will not be affected.

4. SIMULATION VERIFICATION

Simulation results are presented in this section to verify the derived SOC estimation errors under sensing noises for the Kalman filter and its nonlinear extension, EKF. First, a Kalman filter based on a linear battery model with constant OCV slope is simulated to verify (22) directly, which is derived under the linear assumption. The simulation is then extended to EKF and a nonlinear battery model to investigate how accurately (22) could capture the error characteristics under the nonlinear reality.

4.1 Simulation Set-up

The equivalent circuit model of a LiNiMnCo (Li-NMC) battery is used for simulation. This model has been parametrized by Samad et al. (2014), and the parameter values are listed in table 1. The open circuit voltage and its gradient α are also shown in Fig. 2. The OCV profile can be approximated as piecewise linear. When SOC is above 10%, the OCV slope is close to a constant of $\alpha = 0.65V/100\%SOC$.

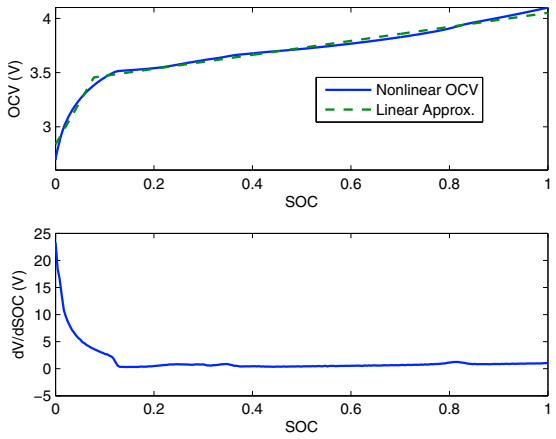

Fig. 2. Open Circuit Voltage Profile and Its Gradient of Li-NMC Battery

4.2 Simulation of Kalman filter and Linear Model

The Kalman filter is examined first for the linear battery model, i.e. the battery OCV is treated as linear.

During simulation, the initial SOC is set to 100%. A constant discharging current of $5A$ is applied for 2800 seconds, giving a final SOC of 22.2%. The SOC swing falls within the near-linear $10\% - 100\%$ range (as shown in Fig. 2), and hence the constant $\alpha = 0.65V/100\%SOC$ is adopted for data generation as well as in the model used by Kalman filter. Noises with $\Delta V = 10mV$, $\sigma_V = 10mV$, $\Delta I = 0.2A$, and $\sigma_I = 0.2A$ are added to the voltage and current profiles to generate the noisy measurement data as shown in Fig. 3. The current sensing variance δI was considered as negligible and hence excluded from the previous derivation. It is included in the simulation here to validate this assumption.

The simulation results are shown in Fig. 4. The dots represent the SOC estimation errors calculated by subtracting the estimated value from the actual value simulated by the model. The blue solid line denotes the derived SOC estimation bias $E(\Delta SOC)$ in (22), and the two dashed lines stand for the derived $E(\Delta SOC) \pm 3\sigma(\Delta SOC)$. It is seen that the actual estimation errors distribute evenly around the derived estimation bias, and mostly within the $\pm 3\sigma(\Delta SOC)$ range. Upon further calculation, the mean actual SOC estimation error over the whole data set is 1.45%, while the derived bias is 1.48%. The actual estimation error standard deviation is 0.15% as compared to the derived value of 0.16%. It can be concluded that the derived estimation error bias and variance match the simulation results closely under the linear model assumption.

Table 1. Model Parameters of Li-MNC Battery (25^oC, 50% SOC)

Parameter	Value
C_{bat}	5 Ah
R_0	2 $m\Omega$
R_1	0.8 $m\Omega$
C_1	6 kF
R_2	1 $m\Omega$
C_2	4 kF

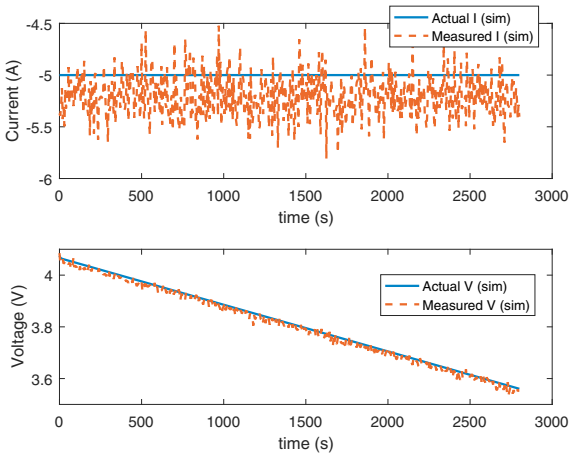

Fig. 3. Current and Voltage Data and Noises Generated from Simulation ($\Delta V = 10mV$, $\sigma_V = 10mV$, $\Delta I = 0.2A$, $\sigma_I = 0.2A$)

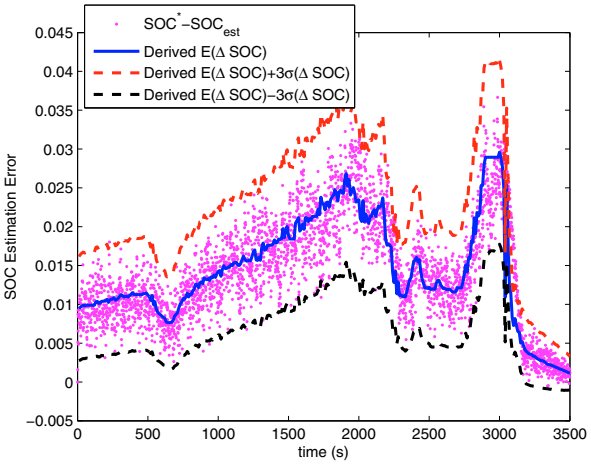

Fig. 5. SOC Estimation Error of EKF for nonlinear model under Sensing Bias and Variance ($\Delta V = 10mV$, $\sigma_V = 10mV$, $\Delta I = 0.2A$, $\sigma_I = 0.2A$)

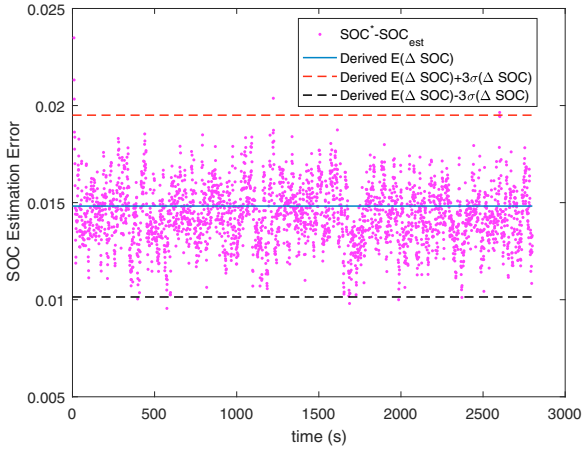

Fig. 4. SOC Estimation Error of KF for Linear Model under Sensing Bias and Variance ($\Delta V = 10mV$, $\sigma_V = 10mV$, $\Delta I = 0.2A$, $\sigma_I = 0.2A$)

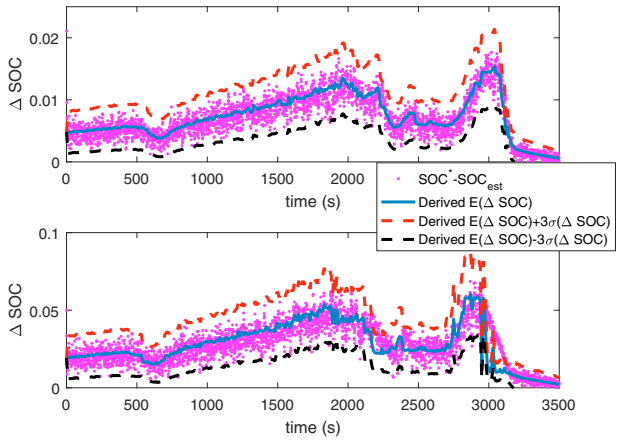

Fig. 6. SOC Estimation Error of EKF under Low and High Sensor Noises (top plot: $\Delta V = \sigma_V = 5mV$, $\Delta I = \sigma_I = 0.1A$; bottom plot: $\Delta V = \sigma_V = 20mV$, $\Delta I = \sigma_I = 0.4A$)

4.3 Simulation of Extended Kalman Filter and Nonlinear Model

The extended Kalman filter is then simulated based on the nonlinear battery model. During simulation, the initial SOC is set to 100%. A constant discharging current of $5A$ is applied for 3500 seconds, giving a final SOC of 2.8%. The original nonlinear OCV curve is used in both data generation and EKF.

Simulated and derived SOC estimation errors are shown in Fig. 5 under noises $\Delta V = \sigma_V = 10mV$ and $\Delta I = \sigma_I = 0.2A$. The derived estimation bias (the blue solid line) is computed based on the equation for $E(\Delta SOC)$ in (22), using time-varying EKF gain K_k and OCV slope α_k evaluated at the estimated SOC. The derived standard deviation is computed based on the equation for $\sigma(\Delta SOC)$ in (22). Based on the comparison to the actual errors, it can be seen that (22) captures the bias and the variance of the estimation error very well, even for this nonlinear case. The actual estimation errors (magenta dots) follow closely the trend predicted by (22): the mean and variance of the errors decrease as the OCV slope increases. It is most obvious after $3000s$ when SOC is below 10% and the OCV slope is large. For further verification, results under two extreme cases of sensor noises are plotted in Fig. 6. The upper plot shows the actual errors and the analytic error bounds under low sensor noises $\Delta V = \sigma_V = 5mV$ and $\Delta I = \sigma_I = 0.1A$, while the bottom plot shows those under high sensor noises, $\Delta V = \sigma_V = 20mV$ and $\Delta I = \sigma_I = 0.4A$. It can be seen that the derived theoretic error bounds capture the actual error spread well mostly in both cases.

5. CONCLUSIONS

The bias and variance of SOC estimation induced by sensor noises are derived analytically in this paper for the Kalman filter based on an equivalent circuit model. The results have been verified by simulation conducted using both the linear and nonlinear battery models.

The analytic expressions could benefit the practice of SOC estimation in the following aspects. First, they can be used to evaluate and predict the SOC estimation accuracy conveniently. It is often extremely difficult, if not impossible, to eradicate the estimation errors caused by inevitable sensing noises in practice. The robustness and reliability of SOC estimation then become critical concerns, which can be evaluated based on the predicted estimation bias and variance. Second, the analytic expressions of the estimation error could aid the observer design process. Traditionally, the Kalman filter needs to assume a known "process noise" to calculate the observer gain. The physical insight of this process noise is unclear, making it hard to determine its covariance. By using the derived error expression, a new observer design method might be proposed to optimize and balance the estimation bias and variance caused by current and voltage sensing noises. The physical significance of sensing noises is easily understood and the noise characteristics can be practically determined.

REFERENCES

Cadirci, Y. and Ozkazanc, Y. (2004). Microcontroller-based on-line state-of-charge estimator for sealed leadacid batteries. *Journal of Power Sources*, 129, 330–342.

Dey, S., Ayalew, B., and Pisu, P. (2015). Nonlinear robust observers for state-of-charge estimation of lithium-ion cells based on a reduced electrochemical model. *IEEE Transactions on Control Systems Technology*, 23, 1935 – 1942.

Domenico, D.D., Stefanopoulou, A., and Fiengo, G. (2010). Lithium-ion battery state of charge and critical surface charge estimation using an electrochemical model-based extended kalman filter. *Journal of Dynamic Systems, Measurement, and Control*, 132, 061302–061313.

Fang, H., Zhao, X., Wang, Y., Sahinoglu, Z., Wada, T., Hara, S., and de Callafon, R.A. (2014). Improved adaptive state-of-charge estimation for batteries using a multi-model approach. *Journal of Power Sources*, 254, 258–267.

Hu, X., Li, S., and Peng, H. (2012). A comparative study of equivalent circuit models for li-ion batteries. *Journal of Power Sources*, 175, 359–367.

Lin, X. (2016). On the analytic accuracy of battery soc, capacity and resistance estimation. In *Proceedings of the American Control Conference*, 4006–4011.

Lin, X., Perez, H., Siegel, J., Stefanopoulou, A., Li, Y., Anderson, R.D., Ding, Y., and Castanier, M. (2013a). Online parameterization of lumped thermal dynamics in cylindrical lithium ion batteries for core temperature estimation and health monitoring. *IEEE Transactions on Control Systems Technology*, 21, 1745–1755.

Lin, X., Perez, H.E., Mohan, S., Siegel, J.B., Stefanopoulou, A.G., Ding, Y., and Castanier, M.P. (2014a). A lumped-parameter electro-thermal model for cylindrical batteries. *Journal of Power Sources*, 257, 1–11.

Lin, X., Stefanopoulou, A., Laskowsky, P., Freudenberg, J., Li, Y., and Anderson, R.D. (2011). State of charge estimation error due to parameter mismatch in a generalized explicit lithium ion battery model. In *ASME Dynamic Systems and Control Conference and Bath/ASME Symposium on Fluid Power and Motion Control*, 393–400.

Lin, X. and Stefanopoulou, A.G. (2015). Analytic bound on accuracy of battery state and parameter estimation. *Journal of The Electrochemical Society*, 162(9), A1879–A1891.

Lin, X., Stefanopoulou, A.G., Li, Y., and Anderson, R.D. (2013b). State of charge estimation of cells in series connection by using only the total voltage measurement. In *Proceedings of the American Control Conference*, 704–709.

Lin, X., Stefanopoulou, A.G., Li, Y., and Anderson, R.D. (2014b). State of charge imbalance estimation for battery strings under reduced voltage sensing. *IEEE Transactions on Control Systems Technology*, 23(3), 1052–1062.

Liu, Z., Ahmed, Q., Zhang, J., Rizzoni, G., and He, H. (2016). Structural analysis based sensors fault detection and isolation of cylindrical lithium-ion batteries in automotive applications. *Control Engineering Practice*, 52, 46–58.

Moura, S.J., Chaturvedi, N.A., and Krstic, M. (2014). Adaptive partial differential equation observer for battery state-of-charge/state-of-health estimation via an electrochemical model. *Journal of Dynamic Systems, Measurement, and Control*, 136(1), 011015–1–8.

Ng, K., Moo, C., Chen, Y., and Hsieh, Y. (2004). Enhanced coulomb counting method for estimating state-of-charge and state-of-health of lithium-ion batteries. *Applied Energy*, 86(9), 1506–1511.

Perez, H. and Moura, S. (2015). Sensitivity-based interval pde observer for battery soc estimation. In *American Control Conference (ACC)*, 323–328. IEEE.

Plett, G.L. (2004). Extended kalman filtering for battery management systems of lipb-based hev battery packs part 3. state and parameter estimation. *Journal of Power Sources*, 134, 277–292.

Plett, G.L. (2011). Recursive approximate weighted total least squares estimation of battery cell total capacity. *Journal of Power Sources*, 196(4), 2319–2331.

Samad, N.A., Siegel, J.B., and Stefanopoulou, A.G. (2014). Parameterization and validation of a distributed coupled electro-thermal model for prismatic cells. In *ASME Dynamic Systems and Control Conference*.

Sharma, A. and Fathy, H.K. (2014). Fisher identifiability analysis for a periodically-excited equivalent-circuit lithium-ion battery model. In *American Control Conference (ACC)*, 274–280. IEEE.

Yuan, S., Wu, H., Ma, X., and Yin, C. (2015). Stability analysis for li-ion battery model parameters and state of charge estimation by measurement uncertainty consideration. *Energies*, 8, 7729–7751.

Zhao, S., Duncan, S.R., and Howey, D.A. (2016). Observability analysis and state estimation of lithium-ion batteries in the presence of sensor biases. *IEEE Transactions on Control Systems Technology*.

Zhao, X. and de Callafon, R. (2013). Data-based modeling of a lithium iron phosphate battery as an energy storage and delivery system. In *American Control Conference (ACC)*, 1908–1913. IEEE.